Why do compact grain boundary complexions prevail in rock-salt materials?

Pierre Hirel, Philippe Carrez, Patrick Cordier

Acta Materialia xxx (xxxx) 118297

Contents lists available at ScienceDirect

Acta Materialia

journal homepage: www.elsevier.com/locate/actamat

Why do compact grain boundary complexions prevail in rock-salt materials?

Pierre Hirel [a,*], Philippe Carrez [a], Patrick Cordier [a,b]

[a] Univ. Lille, CNRS, INRAE, Centrale Lille, UMR 8207 - UMET - Unité Matériaux et Transformations, Lille F-59000, France
[b] Institut Universitaire de France, 1 rue Descartes, Paris F-75005, France

ARTICLE INFO

Article history:
Received 14 March 2022
Received in revised form 27 July 2022
Accepted 22 August 2022

Keywords:
Numerical simulation
MgO
Grain boundary

ABSTRACT

Over 40 years of studies of grain boundaries in ionic rock-salt materials have left the community divided. On one hand, numerical simulations systematically predict open, hollow structural units to be the ground state. On the other, most recent experiments report compact structures to be the norm. To reconcile modelling with experimental evidence, we investigate the stability of three high-angle symmetric tilt grain boundaries in magnesium oxide MgO with respect to the presence of charge-neutral vacancy pairs. We demonstrate that although open structural units are energetically the most favourable, they are easily destabilized by vacancies. It follows that open complexions can never be at equilibrium with the surrounding grains at finite temperature. On the contrary, compact structural units can accommodate a wide range of defects concentrations, and are much more resilient with respect to the absorption of vacancies. These results highlight the limitations of studies that consider only the ground state, and stress the importance of accounting for the presence of other defects when modelling grain boundaries in ionic materials.

1. Introduction

The study of grain boundary (GB) properties in metallic systems has been quite a success story, owing to complementary contributions from numerical simulations and experimental observations. Atomic-scale simulations have long predicted that the ground state for symmetric and asymmetric tilt GBs in face-centred and body-centred metals consists of compact structural units where atoms occupy the GB plane [1–13], and that other compact metastable structures may exist depending on temperature [11,14–17]. These predictions are in excellent agreement with high-resolution observations of GBs in metals [18,19]. Numerical computations also compare well with experimental estimations of GB energies [20], and the mechanisms for their motion including disconnections [10,18,21–23]. All physical properties of GBs derive from their atomic configuration, therefore it is of critical importance that numerical simulations predict GB structures that are relevant and comparable to those observed experimentally.

The situation is more entangled in ionic materials with the rock-salt structure. As early as 1974, Kingery proposed that GBs in sodium chloride NaCl and related compounds may have compact structures similar to those observed in metals [24]. He was contradicted in 1983 when Duffy and Tasker performed atomic-scale simulations in nickel oxide (NiO) [25]. These authors reported that such compact GBs are unstable, and postulated that it was due to electrostatic repulsion between ions of same charge at the interface. Instead they predicted that open, hollow structural units (SU) are the most favourable [25]. This seminal paper obviously had a major influence in the community modelling GBs in oxides, because later simulations systematically have predicted open, hollow SU as the ground-state configuration, using either interionic potentials [26–37], as well as more accurate ab initio calculations [38,39]. More elaborate methods like simulated annealing [35,40] or genetic algorithms [41] also eventually yield open structural units as the ground state, even if they also produce other metastable states that are more compact. The fact that similar open GB structures were predicted by simulations in NaCl [27], NiO [25,26,31], and MgO [29,38,39], indicates that it is a feature shared by many compounds with the rock-salt structure, and quite insensitive to the details of the electronic structure. Based on these numerous and consistent results, many groups restricted their work to the ground-state open complexions as input in their simulations to investigate further GB properties like diffusion [30,42], defect segregation [33,38,43], GB mobility [37] or thermal transport [44]. More compact GB structures are usually found to be unstable or metastable at best, and to be stabilized only in the presence of foreign impurities [45–47] or under very large pressure [35–37,48]. Because they are not the ground state, compact structures have been widely left aside by the modelling community.

These numerical studies are in sharp contrast with the growing body of experiments reporting compact GB structures in rock-salt materials at ambient pressure. As early as 1987, Merkle and Smith reported com-

* Corresponding author.
E-mail address: pierre.hirel@univ-lille.fr (P. Hirel).

https://doi.org/10.1016/j.actamat.2022.118297
1359-6454/© 20XX

pact GB structures in NiO using electron microscopy [49]. More recent high-resolution observations confirmed the compaction of GBs in MgO [46,47,50–53]. These experimental evidences indicate that open complexions seldom occur in real-life samples, and are superseded by more compact structures. This wide discrepancy between experiments and modelling raise quite the conundrum: why do compact complexions prevail over the ground-state open complexions predicted by simulations? The relevance of atomic-scale simulations and their ability to predict realistic GB structures is directly challenged. It is of paramount importance that the modelling community brings a convincing explanation for the prevalence of compact complexions, acknowledge them, and turn its attention to them.

Temperature is naturally one of the major differences between atomistic models and experiments. The former often rely on energy minimization techniques (so-called 0 K calculations), while the latter are bound to finite temperature. Temperature has several effects: it changes the system's free energy via an entropic contribution, and it may introduce lattice disorder due to the formation of thermal vacancies, interstitials, Frenkel or Schottky defects, and so forth. Recently, Yokoi et al. evaluated the role of vibrational entropy in the stability of GBs in MgO with ab initio methods [54]. Their calculations demonstrate that vibrational entropy plays a role on the relative stability of different GBs, and therefore on the expected distribution of GB population. Yet for a given GB disorientation, entropy does not change the relative stability of open complexions over their compact counterpart. As an example, the $\{310\}[001]$ ($\Sigma 5$) GB has the lowest free energy in its open complexion at all temperatures investigated by these authors [54]. We conclude that thermal vibrations alone are insufficient to account for the prevalence of compact GBs.

Another major effect of temperature is the formation of lattice defects, especially at high temperatures. While numerical models usually describe a GB between two perfect, defect-free crystals, natural or synthesized samples often contain other defects like vacancies, interstitials, dislocations, junctions with other GBs, and so on. Previous studies have highlighted the crucial role of vacancies on the stability of GBs in ceria CeO_2 [55] or Y_2O_3-doped ZrO_2 [56]. It is therefore sensible to test the stability of GBs with respect to the presence of vacancies.

The goal of the present study is to rationalize the prevalence of compact GBs, and provide a method for predicting GB structures comparable to observed ones in rock-salt materials. For this, we model three high-angle symmetric tilt grain boundaries (STGB) in MgO at the atomic scale, namely the $\{210\}[001]$ ($\Sigma 5$), $\{310\}[001]$ ($\Sigma 5$), and $\{410\}[001]$ ($\Sigma 17$). First, we show that vacancies are segregated in both open and compact GB configurations. Then, we introduce disorder by gradually removing MgO pairs from the GB, thus breaking symmetry and periodicity in the GB plane. We demonstrate that the open complexions are quickly destabilized and become more compact, while compact complexions accommodate disorder while retaining compact structures.

2. Methods

Magnesium oxide (MgO) with the rock-salt structure is modelled by means of a semi-empirical rigid ion potential, composed of the Coulomb interaction and a Buckingham potential accounting for short-range interactions. We use the parameters proposed by Ball and Grimes as reported by Henkelman et al. [57], with ions charges $q_{\mathrm{Mg}} = -q_{\mathrm{O}} = 1.7\,|e|$ where e is the elementary electric charge. This potential was fitted to ab initio calculations, and was successfully applied to the bulk and surface properties of MgO, to the diffusion of MgO dimer on (100) surface [57], to the study of dislocations [58], of grain boundaries [36], and to the formation energy and migration of Schottky defects [59], demonstrating its transferability and its adequateness for the present study. All simulations are performed with LAMMPS [60]. The Coulomb interaction is computed by means of the particle-particle particle-mesh (pppm) method. The conjugate gradients algorithm is used to minimize the energy, both with respect to atoms positions and the geometry of the simulation cell. In order to allow the system to escape local energy minima, molecular dynamics (MD) simulations are performed at high temperatures (above 1000 K), either in the canonical (NVT) ensemble using a Nosé-Hoover thermostat, or in the isobaric-isothermal (NPT) ensemble using a coupled Nose-Hoover thermostat and barostat. A time step of 1 fs is used to integrate the equations of motion, and durations between 1 ps and 1 ns are simulated. Details of the MD runs depend on the type of simulation, and are specified throughout the results.

Atomic models are constructed with Atomsk [61], as detailed in our previous study [36]. Two grains of MgO are rotated around $Z = [001]$ by opposite angles, resulting in a disorientation α, and then cut and stacked together to produce an initial symmetric tilt grain boundary (STGB). Here we focus on the three following disorientations: $\alpha = 53.1°$ where the two crystals meet with $\{210\}$ planes; $\alpha = 36.8°$ yielding the $\{310\}$ GB; and $\alpha = 28.1°$ corresponding to the $\{410\}$ GB. The resulting systems count about 1000 atoms and contain two equivalent GBs separated by 120 Å, which we verified sufficient to avoid spurious interactions between them. The GB formation energy and excess volume per unit of surface area are respectively defined as:

$$\gamma_h = \frac{E^{\mathrm{GB}} - E^0}{2A}\ , \quad \Omega_h = \frac{V^{\mathrm{GB}} - V^0}{2A} \tag{1}$$

where E^{GB} and V^{GB} are respectively the total energy (eV) and volume (Å^3) of the system containing the GB, E^0 and V^0 the energy and volume of a defect-free system containing the same number of atoms, and A is the area of the GB (Å^2). The factor of 2 accounts for the fact that the simulation cell contains two equivalent GBs. Note that energy differences are always computed between systems counting the same number of atoms. The GB energy per surface area is then expressed in eV Å^{-2} or J m^{-2}, and the excess volume per surface area in Å. Since we only model $\{h10\}[001]$ STGB ($h = 2, 3, 4$) we use the Miller index h as a subscript.

In conservative sampling, the energy landscape is probed by translating the top grain with respect to the bottom one by a vector τ contained in the GB plane, and relaxing atoms only along the direction normal to the GB plane. This method, akin to γ-surface calculations developed for studying dislocations [62], has been widely applied for probing GB structures, both with interionic potentials [28,29,35,36] and with ab initio methods [33,38,39]. Then, for each local minimum found in this landscape, we perform a full relaxation of the ions and the cell with the conjugate-gradients algorithm, in order to reach a stress-free state. The final GB formation energy and excess volume per unit surface area are then defined in Eq. (1).

The energy of interaction between a MgO vacancy pair and the GB is computed as the difference between the total energy E^2 a system where the vacancy pair is in the bulk far from the GB, and the total energy E^1 of a system where the vacancy pair lies inside the GB:

$$E_{\mathrm{int}} = E^2 - E^1 \tag{2}$$

A negative interaction energy means an attractive interaction between the GB and the MgO vacancy pair, while a positive energy means repulsion. When the vacancy pair is introduced far from the GB the interaction energy vanishes, as the energies E^2 and E^1 become more and more comparable. In order to preserve stoichiometry as well as charge neutrality, we remove pairs of MgO vacancies. We verified that the energy of vacancy pairs is lowest by far when the two vacancies sit next to each other along a [001] direction, in agreement with previous studies of Schottky defects in literature [59,63,64]. Therefore, when removing a Mg ion we compute the energies of oxygen vacancies that are first neighbour to it, and remove the O ion where it is most favourable. Then we perform a MD simulation at 1000 K for 10 ps to allow the vacancy

pair to escape an eventual energy minimum and explore other configurations. The GB is duplicated until the interaction energies in the vicinity of the GB are converged within 0.1 eV.

The atomic fraction is varied by sequentially removing pairs of MgO ions from the GB. The vacancy pair concentration n_S is defined as the ratio between the number of MgO units removed and the number of GB structural units (SU) in the periodic cell, $n_S = \left(N_{MgO}\right)/N_{SU}$. It can be related to the atomic fraction ϕ defined as 1− (number of removed atoms)/(number of atoms per layer parallel to the GB) in the works of Frolov et al. [14], or Han et al. [15], and simply quantifies the number of formula units available to construct structural units. After removing a pair of MgO ions we perform MD at 1000 K for 10 ps to allow the system to escape local energy wells, followed by full relaxation of ions and the cell. Then another pair is removed and the procedure is repeated. Since the removal of MgO pairs preserves the stoichiometry, the GB intrinsic energy and volume can still be computed with respect to a reference crystal containing the same number of atoms (Eq. (1)).

Visualization of atomic configurations is performed with OVITO [65]. In order to facilitate the comparison of our atomic configurations with electron microscopy images (*e.g.* HAADF), we also represent our simulated configurations with 2-D Gaussian functions of magnitude proportional to the atomic weight and projected in the (001) plane:

$$f(x,y) = \frac{m}{\sigma\sqrt{2\pi}} \exp\left(-\frac{\left(x-x_0\right)^2 + \left(y-y_0\right)^2}{2\sigma}\right) \tag{3}$$

where m is the mass of an ion and (x,y) its position in the (001) plane, and $\left(x_0,y_0\right)$ the position of the grid element. Projection of atomic configurations into 2-D images is performed with Atomsk [61]. We chose a grid resolution $dx = dy \approx 0.2$ Å and a variance $\sigma = 0.6$ to produce the images.

3. Results

3.1. Conservative sampling of energy landscape

After construction and full relaxation of the initial {210}, {310} and {410} GB configurations, the energy landscape is probed by rigid displacement of a grain by a vector τ contained in the GB plane (conservative sampling). The formation energy γ and excess volume Ω are computed according to Eq. (1). Conservative sampling was already performed in many studies in literature [28,29,33,35,36,38,39], therefore we only briefly describe the results obtained with the current empirical potential.

As an example, the energy map resulting from conservative sampling of the {310} [001] GB is reported in Fig. 1. Only two local energy minima are found, owing to the high symmetry of the GB, in agreement with similar simulations from literature. The first energy minimum is located at $\tau = (0,0)$, and it corresponds to the complexion containing open structural units, illustrated in Fig. 1a. It has an energy $\gamma_3^0 = 1.64$ J m−2 and an excess volume $\Omega_3^0 = 1.28$ Å. The second energy minimum is found by displacing the top grain by half the GB periodicity along X and Z, *i.e.* $\boldsymbol{\tau} = \left(\frac{1}{2},\frac{1}{2}\right)$ in fractional coordinates. It corresponds to the most compact complexion, where structural units are filled with two MgO columns as shown in Fig. 1b. This complexion has an energy $\gamma_3^1 = 1.89$ J m−2 and an excess volume $\Omega_3^1 = 0.69$ Å. The GB energies are comparable to those from literature, for instance Verma and Karki obtained 1.51 and 1.77 J m−2 respectively using ab initio methods [39]. The two energy basins corresponding to these two complexions are separated by very large energies, of the order of 12 eV per unit area. It can be concluded that it is virtually impossible for the system to transform conservatively from one complexion to the other.

The other two GBs yield similar results. For the {210} [001] GB, two energy minima are also found, corresponding to an open complexion ($\gamma_2^0 = 1.47$ J m−2) and a compact complexion ($\gamma_2^1 = 1.87$ J m−2). For the {410} [001] GB we find an energy $\gamma_4^0 = 1.65$ J m−2 for the open complexion, and $\gamma_4^1 = 1.98$ J m−2 for the compact one.

The most important outcomes from conservative sampling are: (1) only two different complexions are found; (2) the open complexion systematically has the lowest energy and is the ground state for all symmetric {h10} [001] GB, regardless of the computation method (DFT or interionic potential); (3) complexions are separated by very large energy barriers, and the system can not transform from one complexion to another in a conservative way. It can be concluded that conservative sampling alone is ill suited for predicting GB complexions that are consistent with experimental observations, and relevant for practical applications.

3.2. Interaction with a MgO vacancy pair

In addition to the previous calculations, it appears necessary to consider non-conservative sampling, i.e. vary the number of atoms present at the interface. To maintain charge neutrality we consider MgO vacancy pairs, and determine if their incorporation into the GB is favourable or not.

To begin, we assess the interaction between the GB and a single MgO vacancy pair, by computing the interaction energy E_{int} between the two defects according to Eq. (2). The initial systems (used previously in conservative sampling) are very small and relied on periodic boundary conditions, so removing a pair of MgO ions from the GB would be equivalent to removing an entire MgO column from each structural unit, which is not a sensible thing to do. As a first step we duplicate the GB so the system contains at least 10 SU along both the X and Z directions, yielding systems containing about 100,000 atoms. We verify that this system size is sufficient to obtain a good convergence of GB energies and interaction energies.

Fig. 2 shows the interaction energy map for each type of GB, both in their open and compact complexions. Mg ions are coloured according to the interaction energy of the associated MgO vacancy pair, while O ions are not coloured (they appear as small white spheres). The interaction maps are symmetric with respect to GB planes, which is expected since we investigate symmetric tilt GBs. Although some sites near the GB planes appear to be unfavourable (represented in red), overall the interaction energies are negative (in blue). This indicates that when a vacancy pair is present, then placing it inside the GB minimizes the system's total energy. Interaction energies are typically larger in magnitude in compact complexions (up to $E_{int} = -3$ eV) than in open complexions (between −1 and −2 eV). These values are consistent with those computed by Uberuaga et al., who reported reduced vacancy formation energies (i.e. attraction) in the vicinity of MgO GBs [33].

At this point it is worth emphasizing that the tendency for vacancy segregation is not associated with a minimization of the GB interface energy. On the contrary, adding defects inside the GB is expected to increase its intrinsic energy (as defined in Eq. (1)), in a similar way that adding defects in a perfect lattice increases its energy. This will be demonstrated in the next section. What the energy maps in Fig. 2 show, is that when a vacancy pair is present, the *system's total energy* is minimized by placing it in the GB. This point is key to understanding the evolution of the GB configuration as more vacancies are added to the system.

3.3. Half-filled columns

Now we remove one pair MgO ions in every second structural unit along the Z = [001] axis, yielding half-filled columns associated with a concentration $n_S = 0.5$/SU. To allow the system to escape local energy minima, a region of 20 Å around the GB is heated at 2000 K and molecular dynamics (MD) is performed in the micro-canonical (NVE) ensem-

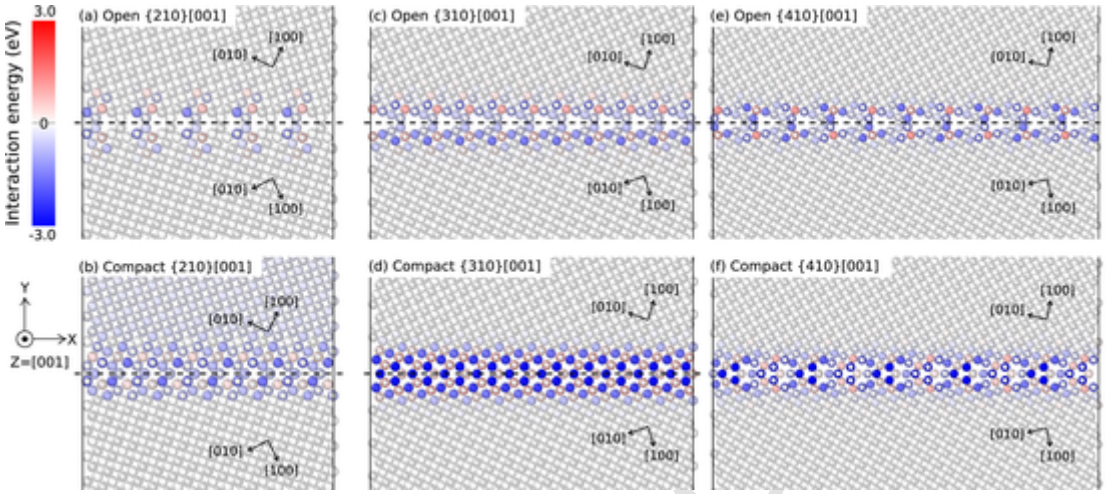

Fig. 2. Atomic configurations and divacancy interaction energy maps for the open (top) and compact (bottom) complexions, for (a,b) the {210}[001] GB ($\alpha = 52.1°$); (c,d) the {310}[001] GB ($\alpha = 36.8°$); (e,f) the {410}[001] GB ($\alpha = 28.1°$). Vertical black lines indicate the boundaries of the simulation cell. Along the [001] direction normal to the page the GB is duplicated 10 times, so each system contains about 100,000 atoms. GB planes are indicated with horizontal dashed lines. Mg ions are coloured according to the interaction energy E_{int} (defined in the text) of the MgO vacancy pair with the GB, blue indicating attractive sites and red negative sites. Oxygen ions are not coloured and simply appear as small white spheres. (For interpretation of the references to colour in this figure legend, the reader is referred to the web version of this article.)

ble for 10 ps, while the remaining ions are maintained fixed to prevent any rigid translation of the grains. This is followed by a full relaxation of atoms and the simulation cell.

Fig. 3 shows the atomic structures obtained after removing half a column from each SU in each of the initial GB. In the open complexions (Fig. 3a,c,e), removal of half columns cause the GBs to relax rapidly into more compact structures. This indicates that open complexions can not contain half-filled columns while remaining open. Instead, atomic columns are displaced inside the GB plane, forming denser SU. The resulting GBs contain MgO columns, some of which are half-filled, i.e.

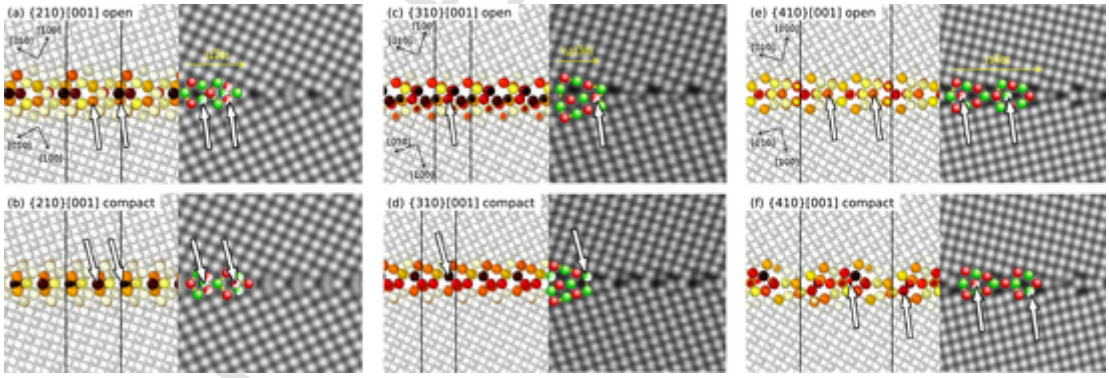

Fig. 3. Atomic configurations of GBs with half-filled columns ($n_S = 0.5$/SU, same colour code as Fig. 1), obtained after removal of half a column in each SU along [001] in (a) the open and (b) compact complexions of the {210} GB; (c) the open and (d) compact complexions of the {310} GB; (e) the open and (f) compact complexions of the {410} GB. White arrows point to the locations of half-filled columns. Gray-scale images are obtained by replacing ions with Gaussian functions (see methods), and SU are overlaid with green and red spheres representing Mg and O ions belonging to the same [001] plane. (For interpretation of the references to colour in this figure legend, the reader is referred to the web version of this article.)

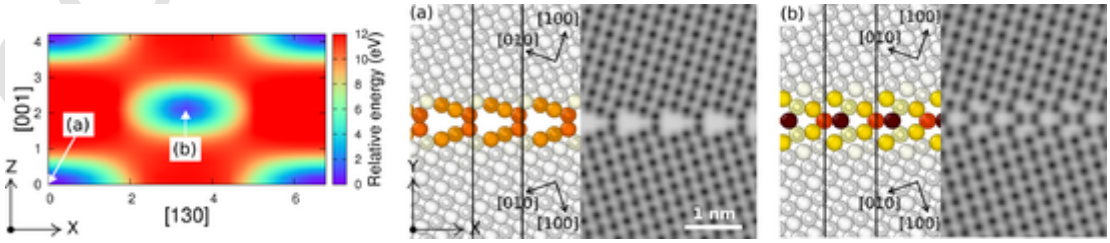

Fig. 1. Surface energy density for the atomically sharp {310}[001]STGB obtained by conservative sampling. The two energy minima correspond to the atomic structures represented on the right-hand side: (a) the ground-state open structural units, often predicted in simulations; (b) metastable compact structural units, more similar to experimental observations. Ions are coloured according to their central symmetry parameter, those in perfect environment being white and those near the GB being coloured. Vertical lines show the boundaries of the actual simulation cell, to which periodic boundary conditions are applied. The gray-scale images are the same configurations where ions are represented as 2-D Gaussian functions (see methods). A structural unit is overlined to facilitate comparison with other GB structures.

every second MgO unit along [001] is missing, as indicated by arrows in Fig. 3.

The intrinsic energies of these configurations are larger than the previous open and compact complexions, and their excess volume is intermediate. For instance, the {310} [001] configuration obtained after removing half columns from the open complexion has an energy $\gamma_3^h = 2.48$ J m^{-2}. It has an excess volume $\Omega_3^h = 0.85$ Å, making it denser than the initial open complexion, but not as much as the fully compact complexion.

In order to facilitate the comparison with experimental observations, we visualized these configuration by replacing atoms with Gaussian functions, as shown in Fig. 3. We find a striking resemblance between our {310} [001] GB (Fig. 3c) and the experimental high-resolution microscopy image obtained by Saito and co-workers [47,51], where SU are filled with three atomic columns. The experimental observation of this configuration confirms its stability. The fact that configurations with half-filled columns are stable and have a well-defined periodicity qualifies them as new complexions of these GBs, distinct from the two discovered with conservative sampling. Note that their periodicity is different from that of the previous open and compact complexions, since along Z the periodicity vector is doubled.

We applied the same procedure to the fully compact GBs, removing half a column and running MD and relaxation. The resulting configurations are shown in Fig. 3b, d and f. Despite the missing half-columns, the SU remain similar to those observed in the fully compact GB (Fig. 2b, d and f). The GBs remain quite compact, with an excess volume comparable to that of the initial compact GB.

These simulations already unveil the different behaviours of the two initial complexions. The open complexions are unstable when they contain half-filled columns, and spontaneously transform into more compact complexions where ions fill the SU. On the contrary, compact complexions accommodate half-filled columns by keeping their SU intact, and they remain compact. This is also reflected in the energy cost associated with the defects: introducing half-filled columns in the open complexion costs about 3.32 eV/SU, while for the compact complexion it is only 1.20 eV/SU.

3.4. Non-conservative sampling

Now we simulate the evolution of the GB when the atomic fraction is varied, i.e. when the number of MgO building blocks available in the GB plane changes gradually. We begin with the open complexion, duplicated to contain 10 SU along X and Z as explained previously. At each iteration, either a pair of MgO ions is removed at a random position near the GB plane, or no ion is removed at all. This allows changing the atomic fraction by increments $\Delta n_S = 0.01$/SU. As previously, a region of 20 Å around the GB is heated at 2000 K and molecular dynamics (MD) is performed, followed by a full relaxation of atoms and the simulation cell. Then another pair of MgO ions is removed and the steps above are repeated. This is similar to the procedure employed by Han and co-workers in metallic systems [15], except that here the τ space is not sampled again after removing ions. The procedure is repeated until a concentration $n_S = 3$/SU is reached, modelling about 1000 different GB configurations for each disorientation, including configurations where the periodicity of the initial GB is not respected. As before, the GB intrinsic energy is defined as the difference of total energy between the system with the GB and a perfect MgO crystal with the same number of atoms (Eq. (1)).

Fig. 4 reports the evolution of the intrinsic energy and volume of each GB as the number of removed MgO units is increased. As stated earlier, the initial GB containing only open SU ($n_S = 0$) has the lowest energy (γ^0) and the largest formation volume (represented in red). As soon as the first ions are removed the GB intrinsic energy increases, as expected from the previous section. What is unexpected is that this energy increases rapidly, reaching $\gamma = 2$ J m^{-2} at the concentration $n_S = 0.13$/SU for all three GB disorientations. Meanwhile, the excess volume drops just as rapidly to $\Omega = 1.12$ Å indicating that the GB becomes much more compact. This evolution is also reflected in the atomic structure of the GB. Fig. 5 shows the atomic configuration of the {310} [001] GB as the concentration of removed ions increases. When $n_S = 0.13$/SU, the GB transforms into a more compact configuration containing a mixture of compact SU and SU with partially filled MgO columns. In other words, removing one MgO pair every eight structural units is sufficient to trigger the transformation into a compact complexion.

As the concentration is increased further, the energy reaches a maximum around 2.2 J m^{-2}, and then remains stable for the {210} [001] GB (Fig. 4), or decreases for the {310} and {410} GBs. Half-filled columns disappear and the SU become more similar to the fully compact complexion, as visible from the atomic configurations (Fig. 5c–e). Concomitantly, as the concentration approaches $n_S = 1$/SU (i.e. when one MgO unit is removed from each SU), the GB intrinsic energy approaches that of the fully compact complexion ($\gamma^1 = 1.89$ J m^{-2}).

As more ions are removed from the GB ($n_S > 1$/SU), its intrinsic energy remains stable in the case of the {210} [001] GB, or increases slightly for the {310} [001] and {410} GBs. However the variations of interface energies are much smaller than the initial increase, and the GB energies vary around 2.2 J m^{-2}. In any case, removing more ions never triggers a transformation back to the open complexion. Instead, the GB keeps a low excess volume (shades of blue in Fig. 4). Inspection of atomic configurations confirms that the GB remains compact, with some atomic columns that are incomplete (Fig. 5g,h). Ultimately, removing more MgO units leads to the migration of the GB out of its plane.

To summarize, open complexions are very sensitive to small variations in the atomic fraction, their interface energy increasing rapidly. Therefore we expect them to be easily destabilized by vacancies, e.g. diffusing from the bulk of the grains or from neighbouring boundaries,

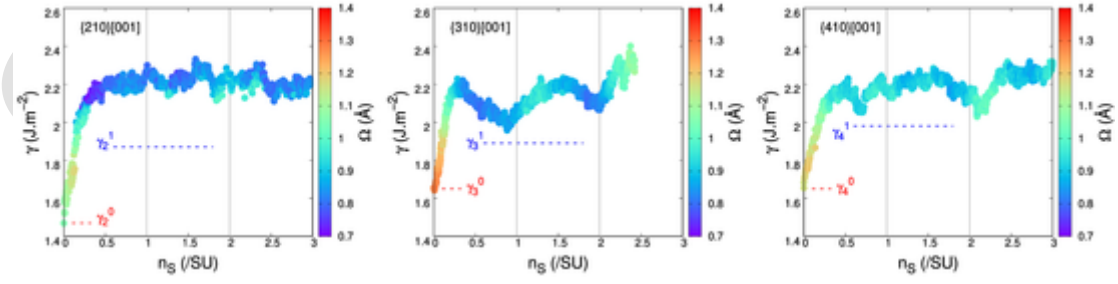

Fig. 4. Evolution of the GB intrinsic energy γ and volume Ω with respect to the concentration of MgO vacancy pairs, for the {210}, {310} and {410} STGB in MgO. The GB excess volume Ω is represented with a colour code, from dark blue (low excess volume, more compact) to red (large volume). The value $n_S = 0$ corresponds to the initial GBs in their open complexion and duplicated $10 \times 1 \times 10$. Several points may correspond to the same value of n_S, because sometimes MD and relaxation are performed without removing any ion. Horizontal dashed lines indicate the energies of the open (γ^0) and compact (γ^1) complexions. (For interpretation of the references to colour in this figure legend, the reader is referred to the web version of this article.)

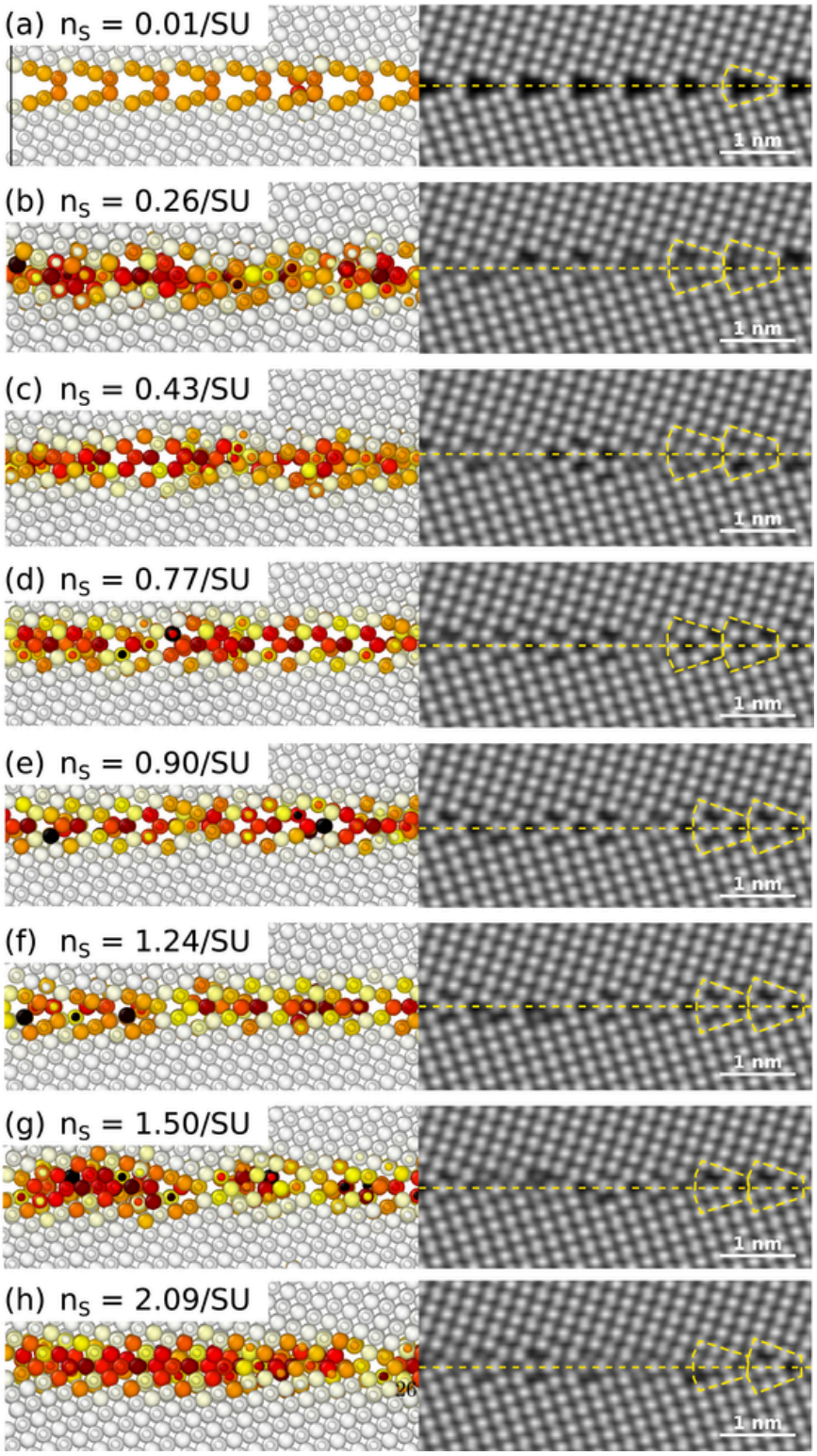

Fig. 5. Evolution of the atomic structure of the {310} [001] GB as pairs of MgO ions are gradually removed from it. Atoms are visualized with the central symmetry parameter (left) and as Gaussian functions (right). The GB plane is overlined with a dashed line. (a) Atomic configuration of the open GB with a single MgO pair removed, corresponding to a concentration $n_S = 0.01/\text{SU}$. The SU are hollow. Following figures correspond to concentrations of (b) $n_S = 0.26/\text{SU}$; (c) $n_S = 0.43/\text{SU}$; (d) $n_S = 0.77/\text{SU}$; (e) $n_S = 0.90/\text{SU}$; (f) $n_S = 1.24/\text{SU}$; (g) $n_S = 1.50/\text{SU}$; (h) $n_S = 2.09/\text{SU}$.

leading them to become more compact. On the contrary, compact configurations are rather insensitive to such variations. They maintain their compaction, and their energy changes are relatively small.

3.5. Defective initial surfaces

In the previous simulations, the initial GBs were constructed from single crystals of MgO with pristine, defect-free surfaces. In experimental work where a GB is formed by stacking two crystals and annealing them at high temperature, it is likely that the initial surfaces are not as regular as the ones typically used in simulations. Instead, each surface may contain steps or terraces, as illustrated in Fig. 6. We investigate the influence of the initial surface state on the type of complexion that is formed when two crystals are joined.

The formation of GBs from defective surfaces is simulated by introducing vacancies in the surfaces of the initial crystals. Mg and O ions are removed from the surfaces at random positions. They do not necessarily form vacancy pairs, but are removed in the same amount to preserve stoichiometry and charge neutrality. Note that the two surfaces, belonging to the top and bottom grains, have different defect concentrations and distributions, and are not mirror images of one another any more. Then the two defective surfaces are brought in contact with each other with the same relative positions as the ones that yielded the open complexions previously, i.e. $\tau = (0, 0)$. All atoms are held fixed, except a region of 20 Å around the GB which is submitted to MD at 2000 K for 100 ps to simulate annealing, followed by minimization. This procedure is illustrated in Fig. 6. At least five different sets of initial defective surfaces are constructed for each disorientation.

Fig. 6 shows typical configurations obtained in the case of the $\{310\}$ GB. The final configuration depends on the initial concentration of vacancies introduced in the free surfaces. For a small number of vacancies (smaller than 0.2 to 0.3/SU), the GB forms in its open complexion where a few columns are defective. For a concentration larger than 0.3/SU, the GB spontaneously adopts a more compact configuration where atomic columns are located inside the GB plane. These compact configurations are comparable to those obtained in the previous section by removing vacancy pairs from an initially open complexion. Similar results were obtained by repeating this procedure with the $\{210\}$ and $\{410\}$ GBs.

In summary, in a bi-crystal where the initial surfaces contain defects (interstitials, vacancies, steps, or terraces), more compact configurations form preferentially. Formation of open complexions appears to require pristine, defect-free surfaces with uninterrupted Mg-O columns along [001], like the one shown in Fig. 6a. Arguably, such well-ordered and defect-free surfaces are unlikely to form in nature or in experiments. As a reminder, it also requires that the two surfaces meet with specific contact points. Indeed, even with pristine initial surfaces, joining the two crystals with a different translation vector may yield the compact complexion anyway, as demonstrated by conservative sampling (Fig. 1).

3.6. Crystallization from a melt

Another important process by which GBs may form, is by crystallization from a melt, when two (or more) crystals nucleate with different crystallographic orientations. We wanted to test if a GB with the open complexion, after melting and quenching, would recover its initial open complexion. We begin with the previous GB structures in their open complexions (duplicated 10 times along X and Z), and freeze atoms in the top and bottom edges of the cell, while the rest of the system is heated for 100 ps at 6000 K, well above the melting temperature. Then the temperature is decreased to 1000 K and MD performed for 1 ns, allowing for the crystals to grow from the frozen top and bottom seeds. A barostat is used throughout the simulation to ensure that the pressure remains close to zero. Finally, atom positions are relaxed in order to investigate the final structures.

Fig. 7 illustrates this procedure, with an example of the $\{310\}\,[001]$ GB. As the system is heated above its melting temperature, the material becomes amorphous and ions diffuse over large distances, especially in the directions of the GB plane. The GB itself cannot be distinguished any more, and is replaced by a thick amorphous region. Then, as temperature is decreased to 1000 K, the material crystallizes rapidly from the frozen top and bottom layers. Typically crystals contain point defects (vacancies and interstitials), however temperature is large enough to allow for significant diffusion, so these defects either annihilate in the bulk, or migrate towards the GB. After 1 ns the system is minimized, and the GB has a compact structure as shown in Fig. 7d and e.

We repeated this procedure at least ten times for each of the three disorientations, melting for 10 to 100 ps, and allowing for up to 1 ns for the crystallization. The details of the atomic structure of the final configuration differs from one run to another. A few vacancies or interstitials may remain trapped inside one grain, the GB may contain partially filled columns, which is understandable given the stochastic nature of MD simulation. However, in all simulations the final GB is always in a compact configuration. After melting and crystallization, the GB never formed spontaneously in the open complexion, not even once. The final configuration does not even contain a single open SU, on the contrary all SU are compact.

While it is true that simulation times are very short, thus limiting diffusion and causing extreme cooling rates, conservative sampling has shown that it is virtually impossible for the system to spontaneously change complexion (Section 3.1). Furthermore, our previous simulations have shown that diffusion of vacancies towards the GB would not transform it into an open complexion. Thus we argue that if open complexions do not form in the limited times accessible with MD, then they are unlikely to form even at longer time scales.

In order to elucidate the role of boundary conditions, we also ran this procedure using smaller cells, containing 10 SU along X but only one along Z. In other words, the periodicity along the $Z = [001]$ axis is imposed to be one lattice vector. In many simulations, after melting and

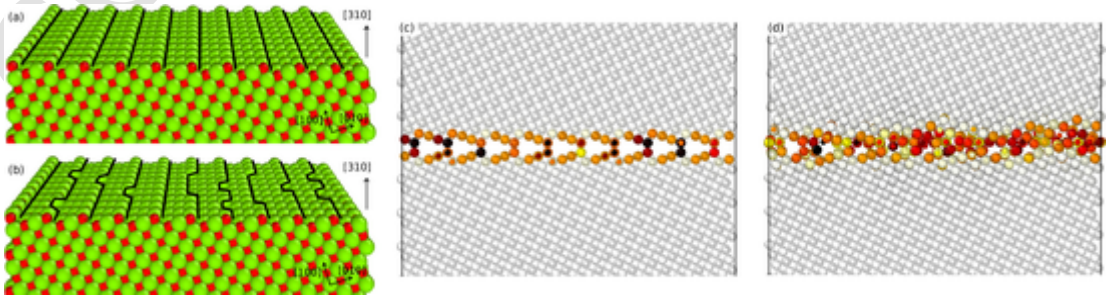

Fig. 6. (a) Crystal of MgO with a pristine, defect-free $\{310\}$ surface, typically used to construct GBs in atomistic simulations. (b) A $\{310\}$ surface containing defects, vacancies and kinks. Contours of the steps are overlaid in black. (c) Two defective surfaces are stacked to form a $\{310\}\,[001]$ GB with open structural units. Note that the system was duplicated 10 times along the Z direction normal to the figure. (d) After MD and relaxation, the GB spontaneously adopts a compact configuration.

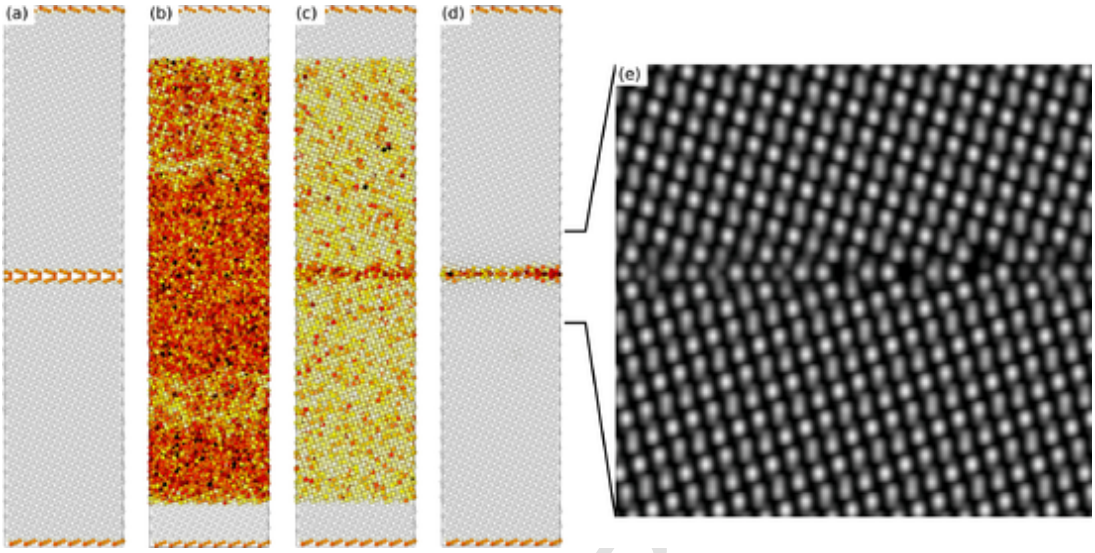

Fig. 7. Simulation of the formation of a {310} [001] GB from a melt. Atoms are coloured according to the centro-symmetry criterion. (a) The initial GB is in the open complexion. Note that it was duplicated 10 times along the Z direction normal to the figure. (b) The system is heated above its melting temperature, at 6000 K. A large portion of the system becomes amorphous. The top and bottom layers (where atoms are displayed as white spheres) remain frozen. (c) Temperature is decreased to 1000 K to allow for crystallization. A GB forms at the center of the cell. (d) After minimization, the GB is in a compact state. (e) Zoom in on the final GB, where atoms are replaced by Gaussian functions (see methods).

crystallization, we observed the spontaneous formation of open structural units. Therefore, it appears that their formation is favoured by imposing a short periodicity to the GB. This is probably why Yokoi and coworkers, although they performed simulated annealing simulations at high temperature, produced GBs with open structural units [35,40]. The preferred open complexions in such simulations can be considered as an artefact due to unrealistically short boundary conditions. Actual GBs in nature or experiments have a large area where ions can diffuse in both directions, and our simulations show that compact complexions are more favoured then.

It is noteworthy that contrary to the previous sections, no atom was added or removed during this procedure. During the melting and subsequent quenching, the number of atoms remains the same as in the original open complexion. We conclude that the absence of vacancies is a necessary but not sufficient condition to the formation of the open complexion. Specific ordering of atoms at the interface seems to be required for the open complexion to form. Enforcing a short periodicity along [001] introduces a bias in the ordering of atomic columns, which seems to facilitate the formation of open configurations. On the contrary when disorder is introduced, e.g. by modelling a larger GB area and using elevated temperature, then more compact GB structures are obtained. We conclude that boundary conditions should be chosen carefully when modelling GBs in ionic materials, so that they do not introduce a bias in the resulting GB structure.

4. Discussion

A GB complexion is commonly defined in literature as a periodic interface, equivalent to a separate phase, which is at equilibrium with its surrounding phases *i.e.* the crystalline grains [66]. Our atomic-scale simulations reveal three different complexions for a STGB in MgO with a given disorientation: one with open structural units, one that is the most compact, and one with half-filled MgO columns. Conservative sampling allows finding only the first two, the latter configuration being accessible only by removing atoms. Just like an MgO crystal containing vacancies is not a new phase, the other GB configurations generated in our study are not complexions, but merely one of the three previous complexions containing vacancies.

Those three complexions were all observed experimentally. The compact complexion of the {210} [001] GB was observed by Bean and co-workers in MgO polycrystals [53]. The compact complexion of the {310} GB with two inner columns can be recognized in the work of Wang et al. in MgO [46], and similar compact SU were also reported in related STGB [45,67]. This compact complexion seems currently to be the most documented one. Yet, the complexion with three inner columns is very similar to the one reported by Saito, Ikuhara and coworkers in a bi-crystal synthesized at high temperature (1500 ◦C for 10 h) [47,51,52]. Our results suggest that one of the inner columns should be half-filled or at least incomplete, however this is difficult to confirm from a 2-D projection of the GB. Finally, the open complexion of the {310} GB was experimentally reported, to the best of our knowledge, only by Kizuka et al. [68]. The scarcity of reports of open complexions in literature indicates that it requires quite specific conditions to be obtained.

By varying the atomic fraction in MgO GBs, we obtain a behaviour that is quite different from that of metals or semiconductors. Frolov et al. studied the influence of the atomic fraction ϕ in face-centered cubic (fcc) copper [14], and Han et al. in fcc aluminium, in body-centred cubic (bcc) tungsten, and in silicon [15]. Starting from a compact GB complexion, they observed that the variations in the GB energies are periodic with respect to variations of ϕ (see e.g. Fig. 8 in Han et al. [15]). Indeed, after removing an entire plane of atoms (i.e. varying ϕ by 1), it is sensible that the GB ends up in a complexion strictly equivalent to the initial one. In MgO we obtain a different behaviour. After varying the atomic fraction gradually up to $n_S = 1$, which is equivalent to removing an entire plane of ions, the GB does not return to an open complexion. Instead it leads to a major increase in GB energy. For larger values of n_S a certain periodicity can be detected for in the {310} and the {410} GBs, corresponding to two equivalent compact complexions ($n_S = 1$ and $n_S = 2$). Just like in metallic and semiconducting systems, cyclic behaviour is only obtained between compact complexions in MgO. During such a cycle the GB never reaches an open complexion.

The occurrence of a GB complexion is not dictated by the ground state, but by thermodynamic equilibrium [69], which is defined by the stability of the system with respect to small perturbations. Although the open GB complexions are associated with the lowest formation energies and hence the ground state, our $\gamma\left(n_S\right)$ curves (Fig. 4) show that they are extremely sensitive to the presence of vacancies: a small variation of n_S results in a large increase of γ and in a rapid compaction, showing that

this complexion is not stable with respect to small variations of the vacancy concentration. Even in pristine MgO, at finite temperature vacancies (or vacancy pairs) are naturally present, and tend to segregate at GBs (as also evidenced by our own calculations in Fig. 2). The fact that the open complexions are so easily destabilized by such defects, means that they cannot be at equilibrium with surrounding grains at finite temperature. This result is key to understanding why the open complexions are so rarely observed in natural or synthesized samples. By contrast, compact complexions endure relatively small variations in their atomic structures, interface energies, and excess volumes, when vacancy pairs are removed from them (Fig. 4). Compact complexions are stable with respect to variations in the chemical potential.

This suggests a critical concentration of vacancies (associated with a critical temperature) below which the open complexion is more stable, and above which compact complexions become more stable, as expected from thermodynamics [69]. It rationalizes the common observations of compact complexion in oxides and suggests that the open complexion, as observed by Kizuka et al. [68], owes to the epitaxial growth on a sodium chloride (NaCl) surface, and the relatively low temperature (300 ◦C) which severely limited vacancy concentration and diffusion.

Scarceness of open complexions can also be understood from a statistical point of view. For a given disorientation, among the thousands of configurations that we sampled (Fig. 4), only a single one corresponds to the open complexion, meaning it has a very low probability of occurrence. Formation of the open complexion requires the whole GB area to form initially with only open structural units (e.g. from pristine, ideal surfaces), and it also requires that no vacancies are absorbed after its formation, because vacancies destabilize open SU (Fig. 4). Such drastic requirements are unlikely to be met in nature or in experiments. By contrast, thousands of configurations that we modelled are compact. These configurations do not require special care in the sample preparation nor any specific ordering, although a few of them do exhibit periodic structural units. Compact configurations are therefore much likely to be obtained, especially when the number of defects at the initial surfaces is uncontrolled, when the sample is prepared at finite temperature, or when the GB was formed after crystallization from a melt.

The present study demonstrates that the presence of defects (vacancies or vacancy pairs) is sufficient to destabilize open complexions, and to favour the formation of more compact configurations. Such mechanisms likely apply to asymmetric tilt grain boundaries as well, where open structural units as described by Yokoi et al. [40] are probably easily destabilized by defects, and more compact structures are reported by experimental observations, like those by Bean et al. [53]. Another important degree of freedom in ionic materials is deviation from stoichiometry. It would be interesting to model the effect of oxygen vacancies on the stability of GB, and on their mobility. Although we focused on MgO as a model ionic material with the rock-salt lattice, we expect our conclusions to be transferable to grain boundaries in other related compounds, including metal oxides (CaO, SrO, BaO, and quite possibly transition metal oxides like CrO, NiO, FeO), fluorides (LiF, NaF, AgF), or chlorides (NaCl, AgCl). Further simulations would be needed to confirm if it is the case. Finally, it is possible that other defects like dislocations, impurities, or junctions with other grain boundaries, would play a similar role and favour compact structures. Such interactions between GBs and other defects remain to be studied.

5. Conclusions

We modelled symmetric tilt grain boundaries in MgO, and investigated the effect of vacancies on the stability of their open and compact complexions. Open GB complexions constitute the ground states for this family of GBs, but can only form when particular conditions are met. In most cases, imperfections at surfaces and interfaces favour the formation of compact GB complexions. After the formation of the initial GB, the segregation of vacancies destabilizes open structural units, thus favouring compact configurations even further. It follows that open complexions are not stable with respect to small variations in the vacancy concentrations inside the grains. These mechanisms provide an explanation to the prevalence of compact GB complexions, as consistently observed in most applications, *e.g.* ceramics synthesized at elevated temperature or rock-salt minerals formed in natural conditions. Studies focusing solely on the open complexion are being sidetracked and probably of little relevance for practical applications. Instead, modelling should focus on compact complexions (most GBs may have more than one), including those containing half-filled or defective columns, in order to bring a better understanding of GBs in rock-salt ceramics and minerals.

Declaration of Competing Interest

The authors declare that they have no known competing financial interests or personal relationships that could have appeared to influence the work reported in this paper.

Acknowledgements

This project has received funding from the European Research Council (ERC) under the European Union's Horizon 2020 research and innovation programme under grant agreement no. 787198 - TimeMan. Computational resources were provided by the DSI at University of Lille.

References

[1] S.P. Chen, D.J. Srolovitz, A.F. Voter, Computer simulation on surfaces and [001] symmetric tilt grain boundaries in Ni, Al, and Ni_3Al, J. Mater. Res. 4 (1) (1989) 62–77, https://doi.org/10.1557/JMR.1989.0062. URL https://www.cambridge.org/core/product/identifier/S0884291400004052/type/journal_article

[2] G. Lu, N. Kioussis, Interaction of vacancies with a grain boundary in aluminum: a first-principles study, Phys. Rev. B 64 (2) (2001) 1–7, https://doi.org/10.1103/PhysRevB.64.024101. arXiv:0101397

[3] D.E. Spearot, K.I. Jacob, D.L. McDowell, Nucleation of dislocations from [0 0 1] bicrystal interfaces in aluminum, Acta Mater. 53 (13) (2005) 3579–3589, https://doi.org/10.1016/j.actamat.2005.04.012.

[4] J.W. Cahn, Y. Mishin, A. Suzuki, Coupling grain boundary motion to shear deformation, Acta Mater. 54 (19) (2006) 4953–4975, https://doi.org/10.1016/j.actamat.2006.08.004.

[5] M.A. Tschopp, D.L. McDowell, Asymmetric tilt grain boundary structure and energy in copper and aluminium, Philos. Mag. 87 (25) (2007) 3871–3892, https://doi.org/10.1080/14786430701455321.

[6] M.A. Tschopp, K.N. Solanki, F. Gao, X. Sun, M.A. Khaleel, M.F. Horstemeyer, Probing grain boundary sink strength at the nanoscale: energetics and length scales of vacancy and interstitial absorption by grain boundaries in α-Fe, Phys. Rev. B 85 (6) (2012) 1–21, https://doi.org/10.1103/PhysRevB.85.064108.

[7] X.M. Bai, L.J. Vernon, R.G. Hoagland, A.F. Voter, M. Nastasi, B.P. Uberuaga, Role of atomic structure on grain boundary-defect interactions in Cu, Phys. Rev. B 85 (21) (2012) 1–10, https://doi.org/10.1103/PhysRevB.85.214103.

[8] A. Rajabzadeh, F. Mompiou, M. Legros, N. Combe, Elementary mechanisms of shear-coupled grain boundary migration, Phys. Rev. Lett. 110 (26) (2013) 1–5, https://doi.org/10.1103/PhysRevLett.110.265507.

[9] B.P. Uberuaga, L.J. Vernon, E. Martinez, A.F. Voter, The relationship between grain boundary structure, defect mobility, and grain boundary sink efficiency, Sci. Rep. 5 (2015) 1–9, https://doi.org/10.1038/srep09095.

[10] N. Combe, F. Mompiou, M. Legros, Disconnections kinks and competing modes in shear-coupled grain boundary migration, Phys. Rev. B 93 (2) (2016) 024109, https://doi.org/10.1103/PhysRevB.93.024109.

[11] N. Chen, L.L. Niu, Y. Zhang, X. Shu, H.B. Zhou, S. Jin, G. Ran, G.H. Lu, F. Gao, Energetics of vacancy segregation to [100] symmetric tilt grain boundaries in bcc tungsten, Sci. Rep. 6 (2016) 1–12, https://doi.org/10.1038/srep36955.

[12] L.L. Niu, Y. Zhang, X. Shu, F. Gao, S. Jin, H.B. Zhou, G.H. Lu, Shear-coupled grain boundary migration assisted by unusual atomic shuffling, Sci. Rep. 6 (March) (2016) 1–9, https://doi.org/10.1038/srep23602.

[13] A.T. AlMotasem, T. Huminiuc, T. Polcar, Factors controlling segregation tendency of solute Ti, Ag and Ta into different symmetrical tilt grain boundaries of tungsten: first-principles and experimental study, Acta Mater. 211 (2021) 116868, https://doi.org/10.1016/j.actamat.2021.116868.

[14] T. Frolov, D.L. Olmsted, M. Asta, Y. Mishin, Structural phase transformations in metallic grain boundaries, Nat. Commun. 4 (May) (2013) 1–7, https://doi.org/10.1038/ncomms2919, arXiv:1211.1756.

[15] J. Han, V. Vitek, D.J. Srolovitz, Grain-boundary metastability and its statistical properties, Acta Mater. 104 (2016) 259–273, https://doi.org/10.1016/

j.actamat.2015.11.035.
[16] J. Han, V. Vitek, D.J. Srolovitz, The grain-boundary structural unit model redux, Acta Mater. 133 (2017) 186–199, https://doi.org/10.1016/j.actamat.2017.05.002.
[17] A.D. Banadaki, M.A. Tschopp, S. Patala, An efficient monte carlo algorithm for determining the minimum energy structures of metallic grain boundaries, Comput. Mater. Sci. 155 (September) (2018) 466–475, https://doi.org/10.1016/j.commatsci.2018.09.017, arXiv:1805.10349.
[18] Q. Zhu, S.C. Zhao, C. Deng, X.H. An, K.X. Song, S.X. Mao, J.W. Wang, In situ atomistic observation of grain boundary migration subjected to defect interaction, Acta Mater. 199 (2020) 42–52, https://doi.org/10.1016/j.actamat.2020.08.021.
[19] T. Meiners, T. Frolov, R.E. Rudd, G. Dehm, C.H. Liebscher, Observations of grain-boundary phase transformations in an elemental metal, Nature 579 (7799) (2020) 375–378, https://doi.org/10.1038/s41586-020-2082-6.
[20] G.S. Rohrer, E.A. Holm, A.D. Rollett, S.M. Foiles, J. Li, D.L. Olmsted, Comparing calculated and measured grain boundary energies in nickel, Acta Mater. 58 (15) (2010) 5063–5069, https://doi.org/10.1016/j.actamat.2010.05.042.
[21] J.P. Hirth, R.C. Pond, Steps, dislocations and disconnections as interface defects relating to structure and phase transformations, Acta Mater. 44 (12) (1996) 4749–4763, https://doi.org/10.1016/S1359-6454(96)00132-2.
[22] S.L. Thomas, K. Chen, J. Han, P.K. Purohit, D.J. Srolovitz, Reconciling grain growth and shear-coupled grain boundary migration, Nat. Commun. 8 (1) (2017) 1–12, https://doi.org/10.1038/s41467-017-01889-3.
[23] Q. Zhu, G. Cao, J. Wang, C. Deng, J. Li, Z. Zhang, S.X. Mao, In situ atomistic observation of disconnection-mediated grain boundary migration, Nat. Commun. 10 (1) (2019) 1–8, https://doi.org/10.1038/s41467-018-08031-x.
[24] W.D. KINGERY, Plausible concepts necessary and sufficient for interpretation of ceramic grain-boundary phenomena: II, solute segregation, grain-boundary diffusion, and general discussion, J. Am. Ceram. Soc. 57 (2) (1974) 74–83, https://doi.org/10.1111/j.1151-2916.1974.tb10818.x.
[25] D.M. Duffy, P.W. Tasker, Computer simulation of ⟨001⟩ tilt grain boundaries in nickel oxide, Philos. Mag. A 47 (6) (1983) 817–825, https://doi.org/10.1080/01418618308243121.
[26] D.M. Duffy, P.W. Tasker, The calculated properties of grain boundaries in nickel oxide.
[27] L.Q. Chen, G. Kalonji, Finite temperature structure and properties of $\Sigma = 5\,(310)$ tilt grain boundaries in nacl a molecular dynamics study, Philos. Mag. A 66 (1) (1992) 11–26, https://doi.org/10.1080/01418619208201510.
[28] G.W. Watson, E.T. Kelsey, N.H. De Leeuw, D.J. Harris, S.C. Parker, Atomistic simulation of dislocations, surfaces and interfaces in MgO, J. Chem. Soc. - Faraday Trans. 92 (3) (1996) 433–438, https://doi.org/10.1039/ft9969200433.
[29] D.J. Harris, G.W. Watson, S.C. Parker, Atomistic simulation of the effect of temperature and pressure on the [001] symmetric dit grain boundaries of MgO, Philos. Mag. A 74 (2) (1996) 407–418, https://doi.org/10.1080/01418619608242151.
[30] D. Harris, G. Watson, S. Parker, Vacancy migration at the (410)[001] symmetric tilt grain boundary of MgO: an atomistic simulation study, Phys. Rev. B 56 (18) (1997) 11477–11484, https://doi.org/10.1103/PhysRevB.56.11477.
[31] J.H. Harding, D.J. Harris, S.C. Parker, Computer simulation of general grain boundaries in rocksalt oxides, Phys. Rev. B 60 (4) (1999) 2740–2746, https://doi.org/10.1103/PhysRevB.60.2740.
[32] D.J. Harris, J.H. Harding, G.W. Watson, Computer simulation of the reactive element effect in NiO grain boundaries, Acta Mater. 48 (12) (2000) 3039–3048, https://doi.org/10.1016/S1359-6454(00)00131-2.
[33] B.P. Uberuaga, X.M. Bai, P.P. Dholabhai, N. Moore, D.M. Duffy, Point defect-grain boundary interactions in MgO: an atomistic study, J. Phys. 25(35). 10.1088/0953-8984/25/35/355001.
[34] S. Kikuchi, H. Oda, S. Kiyohara, T. Mizoguchi, Bayesian optimization for efficient determination of metal oxide grain boundary structures, Phys. B 532 (December 2016) (2018) 24–28, https://doi.org/10.1016/j.physb.2017.03.006.
[35] T. Yokoi, M. Yoshiya, Atomistic simulations of grain boundary transformation under high pressures in MgO, Phys. B 532 (December 2016) (2018) 2–8, https://doi.org/10.1016/j.physb.2017.03.014.
[36] P. Hirel, G.G.F.B.G. Moladje, P. Carrez, P. Cordier, Systematic theoretical study of [001] symmetric tilt grain boundaries in MgO from 0 to 120 GPa, Phys. Chem. Miner. 46 (1) (2019) 37–49, https://doi.org/10.1007/s00269-018-0985-7.
[37] J. van Driel, G. Schusteritsch, J.P. Brodholt, D.P. Dobson, C.J. Pickard, The discontinuous effect of pressure on twin boundary strength in MgO, Phys. Chem. Miner. 47(2). 10.1007/s00269-019-01079-1
[38] K.P. McKenna, A.L. Shluger, First-principles calculations of defects near a grain boundary in MgO, Phys. Rev. B 79 (22) (2009) 1–11, https://doi.org/10.1103/PhysRevB.79.224116.
[39] A.K. Verma, B.B. Karki, First-principles simulations of MgO tilt grain boundary: structure and vacancy formation at high pressure, Am. Mineral. 95 (7) (2010) 1035–1041, https://doi.org/10.2138/am.2010.3386.
[40] T. Yokoi, Y. Kondo, K. Ikawa, A. Nakamura, K. Matsunaga, Stable and metastable structures and their energetics of asymmetric tilt grain boundaries in MgO: a simulated annealing approach, J. Mater. Sci. 56 (4) (2021) 3183–3196, https://doi.org/10.1007/s10853-020-05488-4.
[41] A.B. Mazitov, A.R. Oganov, Grain boundaries in minerals: atomic structure, phase transitions, and effect on strength of polycrystals, Zap. RMO (Proc. Russ. Mineral. Soc.) CL (5) (2021) 92–102, https://doi.org/10.31857/S086960552105004X.
[42] F. Landuzzi, L. Pasquini, S. Giusepponi, M. Celino, A. Montone, P.L. Palla, F. Cleri, Molecular dynamics of ionic self-diffusion at an MgOgrain boundary, J. Mater. Sci. 50 (6) (2015) 2502–2509, https://doi.org/10.1007/s10853-014-8808-9.
[43] B.B. Karki, D.B. Ghosh, A.K. Verma, First-principles prediction of pressure-enhanced defect segregation and migration at MgO grain boundaries, Am. Mineral. 100 (5–6) (2015) 1053–1058, https://doi.org/10.2138/am-2015-5143.
[44] S. Fujii, T. Yokoi, M. Yoshiya, Atomistic mechanisms of thermal transport across symmetric tilt grain boundaries in MgO, Acta Mater. 171 (2019) 154–162, https://doi.org/10.1016/j.actamat.2019.04.009.
[45] Y. Yan, M.F. Chisholm, G. Duscher, A. Maiti, S.J. Pennycook, S.T. Pantelides, Impurity-induced structural transformation of a MgOgrain boundary, Phys. Rev. Lett. 81 (17) (1998) 3675–3678, https://doi.org/10.1103/PhysRevLett.81.3675.
[46] Z. Wang, M. Saito, K.P. McKenna, L. Gu, S. Tsukimoto, A.L. Shluger, Y. Ikuhara, Atom-resolved imaging of ordered defect superstructures at individual grain boundaries, Nature 479 (7373) (2011) 380–383, https://doi.org/10.1038/nature10593.
[47] M. Saito, Z. Wang, Y. Ikuhara, Selective impurity segregation at a near-σ5 grain boundary in MgO, J. Mater. Sci. 49 (11) (2014) 3956–3961, https://doi.org/10.1007/s10853-014-8016-7.
[48] D.J. Harris, G.W. Watson, S.C. Parker, Computer simulation of pressure-induced structural transitions in MgO [001] tilt grain boundaries, Am. Mineral. 84 (1–2) (1999) 138–143, https://doi.org/10.2138/am-1999-1-215.
[49] K.L. Merkle, D.J. Smith, Atomic structure of symmetric tilt grain boundaries in NiO, Phys. Rev. Lett. 59 (25) (1987) 2887–2890, https://doi.org/10.1103/PhysRevLett.59.2887.
[50] D. Vingurt, D. Fuks, M.V. Landau, R. Vidruk, M. Herskowitz, Grain boundaries at the surface of consolidated MgOnanocrystals and acid-base functionality, Phys. Chem. Chem. Phys. 15 (35) (2013) 14783–14796, https://doi.org/10.1039/c3cp51086g.
[51] M. Saito, Z. Wang, S. Tsukimoto, Y. Ikuhara, Local atomic structure of a near-σ5 tilt grain boundary in MgO, J. Mater. Sci. 48 (16) (2013) 5470–5474, https://doi.org/10.1007/s10853-013-7340-7.
[52] K. Inoue, M. Saito, Z. Wang, M. Kotani, Y. Ikuhara, The decomposition formula of 001 symmetrical tilt grain boundaries, Mater. Trans. 56 (12) (2015) 1945–1952, https://doi.org/10.2320/matertrans.M2015277.
[53] J.J. Bean, M. Saito, S. Fukami, H. Sato, S. Ikeda, H. Ohno, Y. Ikuhara, K.P. McKenna, Atomic structure and electronic properties of MgOgrain boundaries in tunnelling magnetoresistive devices, Sci. Rep. 7 (April) (2017) 1–9, https://doi.org/10.1038/srep45594.
[54] T. Yokoi, Y. Arakawa, K. Ikawa, A. Nakamura, K. Matsunaga, Dependence of excess vibrational entropies on grain boundary structures in MgO: a first-principles lattice dynamics, Phys. Rev. Mater. 4 (2) (2020) 26002, https://doi.org/10.1103/PhysRevMaterials.4.026002.
[55] H. Hojo, T. Mizoguchi, H. Ohta, S.D. Findlay, N. Shibata, T. Yamamoto, Y. Ikuhara, Atomic structure of a CeO2 grain boundary: the role of oxygen vacancies, Nano Lett. 10 (11) (2010) 4668–4672, https://doi.org/10.1021/nl1029336.
[56] T. Oyama, M. Yoshiya, H. Matsubara, K. Matsunaga, Numerical analysis of solute segregation at (310)[001] symmetric tilt, Phys. Rev. B 71 (22) (2005) 224105, https://doi.org/10.1103/PhysRevB.71.224105.
[57] G. Henkelman, B.P. Uberuaga, D.J. Harris, J.H. Harding, N.L. Allan, MgO addimer diffusion on MgO(100): a comparison of ab initio and empirical models, Phys. Rev. B 72 (11) (2005) 1–8, https://doi.org/10.1103/PhysRevB.72.115437.
[58] P. Carrez, J. Godet, P. Cordier, Atomistic simulations of 1/2 ⟨110⟩ screw dislocation core in magnesium oxide, Comput. Mater. Sci. 103 (2015) 250–255, https://doi.org/10.1016/j.commatsci.2014.10.019. URL http://linkinghub.elsevier.com/retrieve/pii/S0927025614006934
[59] S. Mahmoud, P. Carrez, M. Landeiro, D. Reis, N. Mousseau, P. Cordier, Diffusion mechanism of bound Schottky defect in magnesium oxide, Phys. Rev. Mater. 5 (3) (2021) 33609, https://doi.org/10.1103/PhysRevMaterials.5.033609.
[60] S.J. Plimpton, Fast parallel algorithms for short-range molecular dynamics, J. Comput. Phys. 117 (1995) 1–19. URL http://lammps.sandia.gov
[61] P. Hirel, Atomsk: a tool for manipulating and converting atomic data files, Comput. Phys. Commun. 197 (2015) 212–219, https://doi.org/10.1016/j.cpc.2015.07.012.
[62] V. Vitek, Intrinsic stacking faults in body-centered cubic crystals, Philos. Mag. 18 (1968) 773–786.
[63] C.A. Gilbert, R. Smith, S.D. Kenny, Ab-initio modelling of defects in MgO, Nucl. Instrum. Methods Phys. Res. Sect. B 255 (1 SPEC. ISS) (2007) 166–171, https://doi.org/10.1016/j.nimb.2006.11.044.
[64] O. Runevall, N. Sandberg, Self-diffusion in MgOa density functional study, J. Phys. 23(34). 10.1088/0953-8984/23/34/345402
[65] A. Stukowski, K. Albe, Dislocation detection algorithm for atomistic simulations, Model. Simul. Mater. Sci. Eng. 18 (2010) 25016.
[66] P.R. Cantwell, M. Tang, S.J. Dillon, J. Luo, G.S. Rohrer, M.P. Harmer, Grain boundary complexions, Acta Mater. 62 (1) (2014) 1–48, https://doi.org/10.1016/j.actamat.2013.07.037.
[67] D. Yin, C. Chen, M. Saito, K. Inoue, Y. Ikuhara, Ceramic phases with one-dimensional long-range order, Nat. Mater. 18 (1) (2019) 19–23, https://doi.org/10.1038/s41563-018-0240-0.
[68] T. Kizuka, M. Ijima, N. Tanaka, Atomic process of electron-irradiation-induced grain-boundary migration in a MgO tilt boundary, Philos. Mag. A 77 (2) (1998) 413–422, https://doi.org/10.1080/01418619808223761.
[69] P.R. Cantwell, T. Frolov, T.J. Rupert, A.R. Krause, C.J. Marvel, G.S. Rohrer, J.M. Rickman, M.P. Harmer, Grain boundary complexion transitions, Annu. Rev. Mater. Res. 50 (2020) 465–492, https://doi.org/10.1146/annurev-matsci-081619-114055.